J Mater Sci (2010) 45:733–743
DOI 10.1007/s10853-009-3992-8

# On the kinetics of nucleation and growth reactions in inhomogeneous systems

**Massimo Tomellini**

Received: 25 June 2009 / Accepted: 23 October 2009 / Published online: 10 November 2009


**Abstract** Nucleation and growth kinetics in systems with a small degree of inhomogeneity are usually modeled through the KJMA (Kolmogorov–Johnson–Mehl–Avrami) theory, that is by using the local values of the nucleation and growth rates which are proper to the region where the transition takes place. In this study, a general expression for the kinetics is derived which applies, in principle, to any degree of inhomogeneity and conforms to previous approaches. The model is employed to study, analytically, first order corrections to the KJMA formula in the case of simultaneous nucleation and interface-limited growth. It is shown that under these circumstances, the nucleus shape is a circle (two-dimensional) whose center is displaced with respect to the point where the nucleation event occurs. The displacement of the center and the radius of the nucleus are both functions of time. The behavior of the Avrami exponent and the impingement factor as a function of the fraction of transformed volume is investigated and discussed.

## Introduction

Reactions in the solid state may proceed by nucleation and growth of the product phase. Typical examples include the precipitation of a new phase from supersaturated solid solution, crystallization of an amorphous system, allotropic transformation, and the initial stage of the oxidation of metal surfaces [1]. The kinetics of the phase transition play an important role in materials science since they affect the microscopic morphology of the sample and, consequently, the mechanical properties of the material [2]. Both theoretical and experimental studies have recently been performed, aimed at an exhaustive characterization of the reactions by studying both the kinetics of the transformed volume and the nucleus size distribution function [3–7].

As far as the kinetics are concerned, that is also the topic of the present contribution, they are usually modeled by means of the celebrated Kolmogorov–Johonson–Mehl–Avrami (KJMA) theory [8–11] which applies under specific conditions, the most well-known of which concern the spatial distribution of the nuclei that is required to be random. It is just this assumption that makes it possible to solve the kinetic problem in closed form and provides us with an equation particularly manageable for describing experimental data. Nevertheless, several models have been developed for investigating the effect, on the phase transition kinetics, of the breakdown of the hypothesis on which the KJMA theory rests. Specifically, these kinetics account for the non-random distribution of the nuclei [12–14], the shielding effect in anisotropic growth [15–19], the parabolic growth law [14, 20–22], the finite size of the system where the transition takes place [23, 24], the finite number of nuclei [25], and the position dependent nucleation rate [26]. Moreover, it is worth noting that most of these kinetic models have been formulated for systems that are translationally invariant.

With regard to the phase transition kinetics, in inhomogeneous samples the nucleation and growth rates are expected to depend on position within the system. This can be ascribed to either a composition or a temperature gradient throughout the specimen. This situation may occur, for instance, when an alloy is quenched at the aging temperature leading to precipitation phenomena or in alloying caused by surface catalytic reactions followed by atom

M. Tomellini (✉)
Dipartimento di Scienze e Tecnologie Chimiche, Università di Roma Tor Vergata, Via della Ricerca Scientifica, 00133 Rome, Italy
e-mail: tomellini@uniroma2.it

diffusion. In the former case, excess vacancies diffuse to lattice defects where they annihilate. Since the flux of vacancies is coupled to the flux of the alloy elements [1], the rate of the transformation is a function of the position-dependent vacancy concentration.

To take an example, surface catalytic reactions coupled with bulk diffusion processes take place in the complex process called "metal dusting" [27]. To be specific, metal dusting occurs in a carburizing atmosphere, for example one containing hydrocarbons, where the metal surface catalyzes the hydrocarbon decomposition and C atom formation. Then C atoms diffuse into the metal, leading to the formation of a metal–carbon solid solution. In the case of iron, this may imply oversaturation of the Fe–C solid solution and, consequently, the nucleation, and growth of cementite [27]. Under these circumstances, due to the concentration profile of C in the alloy, the phase transformation takes place in an inhomogeneous medium. This means that the nucleation and growth rates depend on both position and time and this could lead to anisotropic growth of the nuclei. In turn, this may imply the occurrence of the above mentioned shielding and overgrowth phenomena.

The effect of inhomogeneity on the kinetics of phase transition has been studied, through a phenomenological kinetic equation, by means of the fitting parameter called the "impingement factor" [28, 29]. In reference [30], the effect of inhomogeneity has also been investigated by assuming the KJMA kinetics to hold, locally, and by computing the overall kinetics by averaging the contributions of all volume elements of the sample. Furthermore, from the kinetics, the behavior of the Avrami exponent can be determined as a function of the fraction of transformed volume [28, 30].

In this work, a study is presented of the kinetics of first order phase transitions, ruled by nucleation and growth, in inhomogeneous systems. The inhomogeneity of the nucleation and growth processes is thought to be linked to a time independent concentration gradient. The modeling is more general than those above quoted, since it does not rest on the computation of the "local" transformed volume by means of the KJMA formula. In fact, in the present approach, the effect of the inhomogeneity is taken into account at the level of the statistical computation required to solve the kinetic problem. The general formulation is further employed to study the kinetics in the case of site saturation and interface-limited growth and, with it, the behavior of both the Avrami exponent and the impingement parameter.

The article is divided as follows. In "Kinetics of the transformed volume" section the expression for the transformed volume is derived by using the concept of extended volume. "Application of the kinetic model" section is devoted to studying the growth law when atom attachment at the nucleus interface is rate determining. In "Kinetics of the transformed volume: site saturation" section the transformed volume and the Avrami exponent are computed in the model case of simultaneous nucleation for two- and three-dimensional growths.

## Kinetics of the transformed volume

A general expression for the kinetics of transformed volumes in phase transformation, taking place in non-uniform systems where nucleation centers are distributed at random, has been reported by Avrami in reference [31]. In the present contribution, a different approach to the same problem is presented which gives the solution in terms of nucleation rate and nucleus growth law. It will also be shown that, through a suitable change of variables, the present kinetics reduce to Avrami's formula.

Let us consider a region of the system where, owing to a concentration gradient, the rates of nucleation and growth depend on position. Moreover, the spatial distribution of nuclei is random. In the following we denote with $I(\tau, \boldsymbol{R})$ the nucleation rate at time $\tau$ and at the position stated by the vector $\boldsymbol{R}$, and with $\frac{\mathrm{d}r}{\mathrm{d}t} = G(\boldsymbol{r}, \boldsymbol{R})$ the growth rate along the $\hat{r}$ direction, where $r$ is the modulus of the vector pointing to the cluster surface. As far as the time dependence of the cluster size is concerned, it is obtained from the growth rate as

$$t - \tau = \int_0^r \frac{1}{G(r', \hat{r}, \boldsymbol{R})} \mathrm{d}r', \tag{1}$$

where $\tau$ is the time at which the nucleus started growing and $\boldsymbol{R}$ is taken as constant. Equation 1 gives the nucleus growth law $r \equiv r(t - \tau, \hat{r}, \boldsymbol{R})$ for a nucleus centred at $\boldsymbol{R}$.

The statistical problem one wants to solve is the following: given a generic point of the system, say at $\boldsymbol{R}_0$, what is the probability that this point be transformed at time $t$ by the new phase. In turn, this probability is just equal to the fraction of transformed volume at $\boldsymbol{R}_0$, $\xi(\boldsymbol{R}_0, t)$. It is worth noting that the dependence of the nucleation and growth rates on position is brought about, for instance, by the non-uniform concentration of the chemical components that rule the reaction.

By denoting with $\mathrm{d}P(\tau, t', \boldsymbol{R}, \boldsymbol{R}_0)$ the probability that the point is transformed in the time interval $\mathrm{d}t'$ around $t'$ by the nucleus born in the time interval $\mathrm{d}\tau$ around $\tau$ and in the volume element $\mathrm{d}\boldsymbol{R}$ around $\boldsymbol{R}$, one gets

$$\mathrm{d}P(\tau, t', \boldsymbol{R}, \boldsymbol{R}_0) = [1 - \xi(\boldsymbol{R}_0, t')] I(\tau, \boldsymbol{R}) \mathrm{d}\tau \mathrm{d}\psi r^n G(-\boldsymbol{r}, \boldsymbol{R}) \mathrm{d}t', \tag{2}$$

where $n = \mathrm{D} - 1$, with D being the space dimension and $\mathrm{d}\psi = \mathrm{d}\theta$ and $\mathrm{d}\psi = \sin\theta \mathrm{d}\phi \mathrm{d}\theta$ for $\mathrm{D} = 2$ and $\mathrm{D} = 3$,

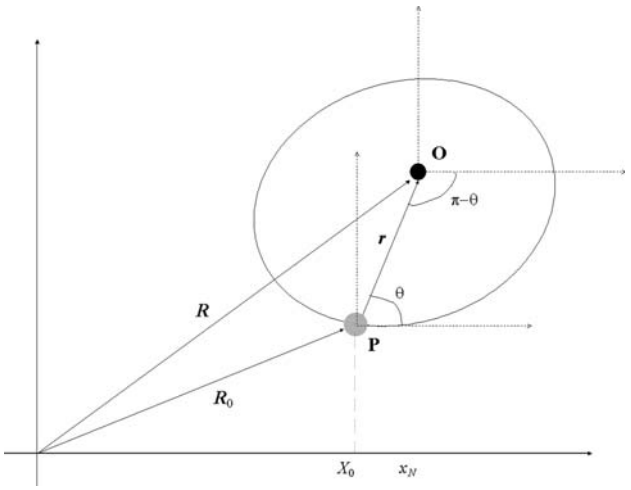


**Fig. 1** Reference frames employed in the computation developed in "Kinetics of the transformed volume". The nucleus center, O (*black symbol*), is located at $\boldsymbol{R}$ and the generic point, P (*grey symbol*), at $\boldsymbol{R}_0$. The local reference frame is centered at O

respectively. In Eq. 2 $\boldsymbol{r} = \boldsymbol{R} - \boldsymbol{R}_0$ and the point, identified by the vector $-\boldsymbol{r}$, lies on the cluster surface (see Fig. 1). In this respect, it is important to emphasize that in Eq. 2 $G$ and $\boldsymbol{R}$ have to be considered functions of $t' - \tau$ and $\psi$. In fact, $G_{2D}(-\boldsymbol{r},\boldsymbol{R}) \equiv G_{2D}(r,\pi+\theta,\boldsymbol{R})$ and $G_{3D}(-\boldsymbol{r},\boldsymbol{R}) \equiv G_{3D}(r,\pi+\phi,\pi-\theta,\boldsymbol{R})$, expressions that are rewritten in a more concise form as $G(-\boldsymbol{r},\boldsymbol{R}) \equiv G(r,\psi',\boldsymbol{R})$ where $\psi' \equiv \psi'(\psi)$ is a function of $\psi$. Therefore, the integration of the growth rate leads to

$$t - \tau = \int_0^r \frac{1}{G(r',\psi',\boldsymbol{R})}\mathrm{d}r'. \tag{3}$$

As above, in Eq. 3 $\boldsymbol{R}$ is independent of the integration variable. According to Eq. 3 one gets the functions $r \equiv g(t-\tau,\psi',\boldsymbol{R}) = g(t-\tau,\psi',\boldsymbol{r}+\boldsymbol{R}_0) = \tilde{g}(t-\tau,\psi',r,\psi,\boldsymbol{R}_0)$ namely an implicit equation for $r$ that can be formally rewritten as

$$r \equiv r(t-\tau,\psi,\boldsymbol{R}_0). \tag{4}$$

The physical meaning of this equation is straightforward: it is the distance that a growing nucleus located at $\boldsymbol{r}+\boldsymbol{R}_0$ covers along the direction $\psi' \equiv \psi'(\psi)$, in the time interval $t-\tau$, $\tau$ being the birth time of the nucleus.

In Eq. 1 the term $[1-\xi(t',\boldsymbol{R}_0)]$ is the probability that the generic point is untransformed at time $t'$ and the nucleation rate is also comprehensive of the contribution of the phantom nuclei. Clearly, Eq. 1 holds true provided that the phantom overgrowth and the shielding process are not allowed [18, 32]. Furthermore, in the case of anisotropic growth, as considered here, the shielding among clusters does not occur provided the orientation is the same for all nuclei [32].

Since the probability that the generic point be transformed in the time interval $\mathrm{d}t'$ around $t'$ is equal to $\mathrm{d}\xi(t',\boldsymbol{R}_0)$, from Eq. 2 it follows that

$$\frac{\mathrm{d}\xi(t',\boldsymbol{R}_0)}{\mathrm{d}t'} = [1-\xi(t',\boldsymbol{R}_0)]\int_{\Delta\psi}\mathrm{d}\psi\int_0^{t'} I(\tau,\boldsymbol{R})r^n G(-\boldsymbol{r},\boldsymbol{R})\mathrm{d}\tau \tag{5}$$

or, by integration,

$$\ln[1-\xi(t,\boldsymbol{R}_0)] = -\int_{\Delta\psi}\mathrm{d}\psi\int_0^{t}\mathrm{d}t'\int_0^{t'} I(\tau,\boldsymbol{R})r^n G(-\boldsymbol{r},\boldsymbol{R})\mathrm{d}\tau, \tag{6}$$

where $\Delta\psi$ denotes the integration domain of the angular variables. It is worth noting that the integrand of Eq. 6 is a function of the integration variables. In fact, in Eq. 6 $\boldsymbol{R} = \boldsymbol{r} + \boldsymbol{R}_0$, $G(-\boldsymbol{r},\boldsymbol{R}) \equiv G(r,\psi',\boldsymbol{R})$ and the nucleus size is given by $r \equiv r(t'-\tau,\psi,\boldsymbol{R}_0)$ (Eq. 4). Equation 6 gives the formal solution of the kinetics for transitions occurring in inhomogeneous systems provided that the phantom overgrowth and the shielding phenomenon are both precluded. Equation 6 is similar to the KJMA formula where the multiple-integral in the second member can be thought as the position-dependent "extended volume".

It is possible to show that Eq. 6 is, in fact, compatible with Avrami's solution [31]. By changing the integration variable from $\tau$ to $r$ and using the identity $\frac{\mathrm{d}\tau}{dr} = -\frac{1}{G}$ (Eq. 1), Eq. 6 becomes

$$\ln[1-\xi(t,\boldsymbol{R}_0)] = -\int_{\Delta\psi}\mathrm{d}\psi\int_0^{t}\mathrm{d}t'\int_0^{r(t',\psi,\boldsymbol{R}_0)} I(\tau(r,t',\psi,\boldsymbol{R}_0),\boldsymbol{r}+\boldsymbol{R}_0)r^n\mathrm{d}r. \tag{7}$$

In Eq. 7 the nucleation time, $\tau$, which enters the nucleation rate, has been expressed in terms of $r$, $t'$ and $\psi$ through the inversion of $r \equiv r(t'-\tau,\psi,\boldsymbol{R}_0)$. Also, the extreme of integration, $r \equiv r(t',\psi,\boldsymbol{R}_0)$, is the distance—from the generic point (P in Fig. 1)—of a nucleus which started growing at $\tau = 0$ and transforms the point P at time $t'$. It is the maximum distance at which a nucleus capable of growing through $\boldsymbol{R}_0$ can lie. Next, by exchanging the order of integration between the $r$ and the $t'$ variables the kinetics becomes (see also Fig. 2a, b)

$$\ln[1-\xi(t,\boldsymbol{R}_0)] = -\int_{\Delta\psi}\mathrm{d}\psi\int_0^{r(t,\psi,\boldsymbol{R}_0)} r^n\mathrm{d}r\int_{t'(r,\psi,\boldsymbol{R}_0)}^{t} I(\tau(r,t',\psi,\boldsymbol{R}_0),\boldsymbol{r}+\boldsymbol{R}_0)\mathrm{d}t', \tag{8}$$

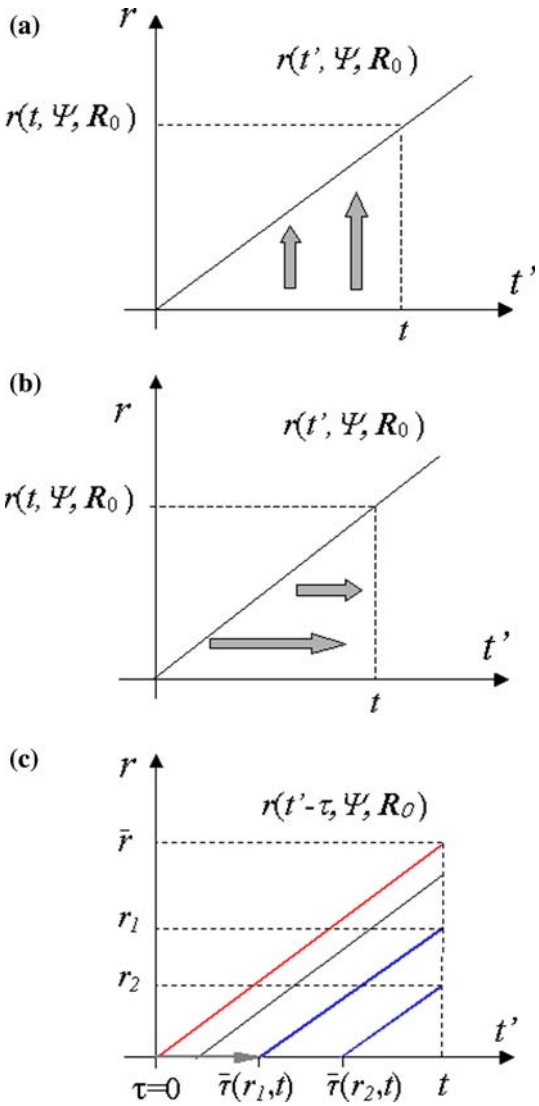


**Fig. 2** Integration domains of the integrals defined in "Kinetics of the transformed volume". Panels **a**, **b**, and **c** refer to Eqs. 7, 8, and 9a, respectively. In panels **a** and **b** a linear growth law, $r(t', \psi, \boldsymbol{R}_0)$, is shown for a nucleus that starts growing at time $\tau = 0$. The *arrows* indicate the $(r, t')$ integration domains of Eq. 7 (panel **a**) and Eq. 8 (panel **b**). In panel (**c**) the growth law, $r(t' - \tau, \psi, \boldsymbol{R}_0)$ is shown as a function of $t'$ and for different values of $\tau$. Specifically, $\bar{\tau}(r_i, \psi, t)$ $(i = 1, 2$; in the figure the $\psi$ variable has been omitted) is the birth time of a nucleus, at $\boldsymbol{r}_i$, which transforms the point at running time $t$. The *solid lines* are the functions $r(t' - \bar{\tau}, \psi, \boldsymbol{R}_0)$. In particular, the *red line* refers to the function $r(t', \psi, \boldsymbol{R}_0)$ that gives the radius of influence $\bar{r} = r(t, \psi, \boldsymbol{R}_0)$. In Eq. 9a the $\tau$ variable spans the range marked by the *arrow*. (Color figure online)

where $t' = t'(r, \psi, \boldsymbol{R}_0)$ is obtained by inverting $r \equiv r(t', \psi, \boldsymbol{R}_0)$. The last integral in Eq. 8 can be further elaborated by noting that at constant $r$, $\mathrm{d}t' = \mathrm{d}\tau$. Accordingly, by changing the variable, Eq. 8 eventually becomes

$$\ln[1 - \xi(t, \boldsymbol{R}_0)] = -\int_{\Delta\psi} \mathrm{d}\psi \int_0^{\bar{r}} r^n \mathrm{d}r \int_0^{\bar{\tau}} I(\tau, \boldsymbol{r} + \boldsymbol{R}_0)\mathrm{d}\tau, \tag{9a}$$

where $\bar{\tau} \equiv \tau(t, r, \psi, \boldsymbol{R}_0)$ is the birth time of a nucleus which transforms the point at running time $t$ and $\bar{r} = r(t, \psi, \boldsymbol{R}_0)$ defines the boundary of the region of influence for the point at $\boldsymbol{R}_0$ (Fig. 2c).

The meaning of Eq. 9a is the following: the term

$$N[\bar{\tau}, \boldsymbol{r}]\mathrm{d}\boldsymbol{r} = \left(\int_0^{\bar{\tau}} I(\tau, \boldsymbol{r} + \boldsymbol{R}_0)\mathrm{d}\tau\right)\mathrm{d}\boldsymbol{r} \tag{9b}$$

is equal to the number of nuclei (phantom included) within $\mathrm{d}\boldsymbol{r}$ which are capable of transforming the generic point up to time $t$. Integration over $\mathrm{d}\boldsymbol{r}$ will eventually give the total number of nuclei which have grown through that point. Inserting Eq. 9b into Eq. 9a gives the solution of reference [31].

## Application of the kinetic model

### Growth law

The simplest application of the kinetics concerns two-dimensional growth in the presence of an unidirectional concentration gradient along, say, the $x$-axis. The concentration of the species is uniform in the $y$ direction. Here, we deal with interface-limited growth where the growth rate is proportional to the concentration of the species at the interface. For the sake of simplicity, the growth is ruled by a single component of the system. In addition, we first discuss the case in which the shape of the nucleus is dictated by the rate of atom attachment at the nucleus surface, i.e., redistribution of matter in the nucleus is kinetically inhibited (type-I mechanism). On the contrary, when atom mobility at the periphery of the nucleus is high, the nucleus shape conforms to the criterion of the energy minimum and becomes independent of growth rate (type-II mechanism). This is the case, for example, of the spherical nucleus for which shape the surface energy term minimizes. Under these circumstances, the computation of the growth law is expected to be simpler for the shape of the nucleus is given a priori. It will be shown, however, that with a small degree of inhomogeneity the two models lead to similar results.

In the absence of matter redistribution the rate equation for the nucleus growth reads[1]

[1] Strictly speaking the evolution of the local curvature of the nucleus, under interface-limited growth, is governed by the equation $\frac{\mathrm{d}\Re}{\mathrm{d}t} = \frac{\partial\Re}{\partial t} + \frac{\partial\Re}{\partial x}v_x \equiv \alpha c(x)$ where $v_x = \frac{\mathrm{d}\Re}{\mathrm{d}t}\hat{n}\hat{x}$ is the local growth rate along $x$ and $\hat{n}$ is the normal to the nucleus surface. Combining these equations one gets $\frac{\partial\Re}{\partial t} = \alpha c(x)\left[1 + \frac{\partial\Re}{\partial x}\frac{\partial y/\partial x}{\sqrt{1+(\partial y/\partial x)^2}}\right]$. Equation 10 holds provided $\partial\Re/\partial x \ll 1$. It can be proved that this condition is fulfilled in the case $r_0/\lambda \ll 1$ here considered.

$$\frac{\partial \Re(x,t)}{\partial t} \cong \alpha c(x) \tag{10}$$

where $\Re(t, x)$ is the local curvature of the nucleus at time $t$, $c(x)$ is the species concentration, $\alpha = av/\rho$ with $a$ and $v$ being the jump distance and hopping frequency, respectively, and $\rho$ is the density of the nucleus. In addition, by employing Cartesian coordinates, the local curvature of the nucleus is linked to the nucleus shape through the expression

$$\Re(t,x) = \frac{(1+\eta^2)^{3/2}}{\left|\frac{\partial \eta}{\partial x}\right|} \tag{11}$$

with $\eta = \frac{\partial y(x,t)}{\partial x}$ and $y(x, t)$ being the equation of the nucleus boundary at time $t$. It is worth noting that since the characteristic length over which the concentration changes is usually shorter than the mean size of the nuclei, approximations can be employed. In particular for the zero-order approximation $c(x) \cong c(x_0)$, where $x_0$ is the coordinate of the nucleus center, Eq. 11 gives a circle. One gets $\Re(t) = r(t, x_0) = \alpha t c(x_0) + r^*$ where at $t = 0$ the nucleus shape is a circle of radius $r^*$, namely the critical radius. In the following, we go beyond the zero-order approximation by including first order corrections to the concentration profile around the nucleus.

In the mathematical computations that follow spatial coordinates are measured with respect to the reference frame located at the nucleus center: $x = x_0 = 0$, $y = y_0 = 0$. Since $c = c(x)$ the growth is symmetric with respect to the $x$-axis. As a consequence, the intersection points between the nucleus boundary and the $x$-axis, $x = \bar{x}(t)$, satisfy the equation

$$\frac{\mathrm{d}\bar{x}(t)}{\mathrm{d}t} = \pm \alpha c(\bar{x}), \tag{12}$$

where the positive and negative signs refer to $\bar{x} > 0$ and $\bar{x} < 0$, respectively. As anticipated above, we take advantage of the fact that the length scale over which the concentration changes is much longer than the mean nucleus size. On this basis, a nucleus located at $x_0$ will grow under a nearly constant concentration gradient as given by the first order expansion

$$c(x) \cong c_0\left(1 - \frac{x}{\lambda}\right), \tag{13}$$

where $\lambda = -\frac{c(x_0)}{c'(x_0)}$ and $c_0 = c(x_0)$. In Eq. 13 $\lambda$, that is a function of $x_0$, is much longer than the mean size of the nuclei. In the case $\left.\frac{\mathrm{d}c}{\mathrm{d}x}\right|_{x_0} = c'(x_0) < 0$ the characteristic length, $\lambda$, is greater than zero. The zero-order approximation is eventually recovered in the limit $\lambda \to \infty$. For $\bar{x} > 0$ Eq. 12 gives

$$c_0 \alpha \tau_{\bar{x}} = -\lambda \ln\left(1 - \frac{\bar{x}}{\lambda}\right) + \lambda \ln\left(1 - \frac{r^*}{\lambda}\right), \tag{14}$$

where $\tau_{\bar{x}}$ is the time at which the nucleus boundary crosses the point $y = 0$, $x = \bar{x}$ and, as already said, we set $x_0 = 0$. For $\bar{x} < 0$ the second member of Eq. 14 has to be multiplied by $-1$. Next we use this result to compute the local curvature $\Re(t, x)$ by integrating Eq. 10 at constant $x$, where the time variable spans the range $\tau_x \div t$. The solution is

$$\Re(t,x) - \Re(\tau_x, x) = \alpha c(x)(t - \tau_x). \tag{15}$$

Using Eqs. 13, 14 and assuming $\Re(\tau_x, x) \approx x$, Eq. 15 becomes (for $x > 0$)

$$\Re(t,x) = x + r_0(t)\left(1 - \frac{x}{\lambda}\right) + \lambda \ln\left(1 - \frac{x}{\lambda}\right) - x \ln\left(1 - \frac{x}{\lambda}\right), \tag{16a}$$

where $r_0(t) = \alpha c_0 t$ and the contribution due to the critical size has been disregarded. In a similar fashion, for $x < 0$ one obtains

$$\Re(t,x) = -x + r_0(t)\left(1 - \frac{x}{\lambda}\right) - \lambda \ln\left(1 - \frac{x}{\lambda}\right) + x \ln\left(1 - \frac{x}{\lambda}\right). \tag{16b}$$

As anticipated, the condition $\frac{r_0(t)}{\lambda} \ll 1$ is considered and this justifies a series expansion in terms of $x/\lambda$ obtaining

$$\Re(t,x) \cong r_0(t) - \frac{r_0(t)}{\lambda}\left(x - \frac{x^2}{2r_0(t)}\right) \quad (x > 0) \tag{16c}$$

and

$$\Re(t,x) \cong r_0(t) - \frac{r_0(t)}{\lambda}\left(x + \frac{x^2}{2r_0(t)}\right) \quad (x < 0). \tag{16d}$$

We are now in a position to determine the shape of the nucleus. Equation 11 is solved for $\eta$ according to

$$\frac{\eta}{(1+\eta^2)^{1/2}} = \pm f \tag{17a}$$

that implies

$$\frac{\mathrm{d}y}{\mathrm{d}x} = \pm \frac{f}{\sqrt{1 - f^2}}, \tag{17b}$$

where

$$f(x,t) = \int_0^x \frac{1}{\Re(w,t)} \mathrm{d}w + K_0 \tag{17c}$$

with $K_0$ as the integration constant (time dependent). By employing Eqs. 16c, 16d into Eq. 17c, and retaining terms up to the first order in $\lambda'^{-1} = r_0(t)/\lambda$, one gets

$$f(x,t) \cong x' + \frac{1}{2\lambda'}x'^2 - \frac{1}{6\lambda'}x'^3 + K_0 \quad (x > 0) \tag{18a}$$

$$f(x,t) \cong x' + \frac{1}{2\lambda'}x'^2 + \frac{1}{6\lambda'}x'^3 + K_0 \quad (x<0) \tag{18b}$$

where $x' = x/r_0(t)$ and the expansion $(1+x)^{-1} \cong 1-x$ was exploited. In addition, using Eq. 17c the solution of Eq. 17b can be recast in the form

$$y = \pm\left[K_1 - \Re\sqrt{1-f^2} + \int \sqrt{1-f^2}\frac{\mathrm{d}\Re}{\mathrm{d}f}\mathrm{d}f\right], \tag{19}$$

where $K_1$ is the integration constant and $\Re(x(f,\ t),\ t)$ is attained by inverting the $f(x,\ t)$ function with respect to $x$. Moreover, since the derivative $\frac{\mathrm{d}\Re}{\mathrm{d}f}$ scales as $\frac{\mathrm{d}\Re}{\mathrm{d}f} \propto \frac{r_0}{\lambda'}$ and $y$ is nil at $f = \pm 1$, it is possible to show that also $K_1 \propto r_0/\lambda'$ and the leading term of Eq. 19 reads

$$y' \cong \pm\sqrt{1-f^2}, \tag{20}$$

where $y' = y/r_0(t)$ and $f(x,\ t)$ is given by Eqs. 18a, 18b. However, to evaluate Eq. 20 the integration constant, $K_0$, has to be estimated. This is accomplished by exploiting the conditions $\Re(\bar{x}) = \pm\bar{x}$ and $f(\bar{x}) = \pm 1$, that is a system of equations, where the minus sign refers to the case $\bar{x}<0$. Specifically, by retaining terms up to the first order in $\lambda'^{-1}$ the solutions of the second order equations $\Re(\bar{x}) = \pm\bar{x}$ read $\bar{x}'_+ = 1 - \frac{1}{2}\lambda'^{-1}$ and $\bar{x}'_- = -\left(1 + \frac{1}{2}\lambda'^{-1}\right)$ with $\bar{x}' = \bar{x}/r_0$. Moreover, the leading term of the expression $f(\bar{x}_+) = 1$ eventually provides $K_0 \cong \lambda'^{-1}/6$.

The shape of the nucleus, as given through Eq. 20, has been displayed in Fig. 3 for several values of the $\lambda'$ parameter. As Fig. 3 shows, the nucleus is more anisotropic the smaller the $\lambda'$. In fact, for $\lambda' > 0$ the growth is faster the smaller the $x$-coordinate of the nucleus boundary. Let us approximate Eq. 20 according to

$$\frac{y(x,t)}{r_0(t)} = \pm\sqrt{1 - \left(\frac{x}{r_0(t)} + \frac{r_0(t)}{2\lambda}\right)^2} \tag{21}$$

namely, the nucleus shape is a circle of radius $r_0(t)$. The *center of the nucleus* is located at $x = y = 0$, whereas the coordinates of the *center of the circle* are $x = -\gamma\frac{r_0^2}{\lambda}$, $y = 0$, where $\gamma = 1/2$. Besides for $\lambda > 0$ the circle center is located at $x < 0$, since the growth is faster at $x < 0$. These "displaced circles" are shown in Fig. 4 where the approximate solution, Eq. 20, has also been reported for comparison. As one can see, the displaced circles represent a good description of the approximate solution of Eq. 20. Under these circumstances the mathematical formulation of the kinetics is simpler and makes it possible to find an analytical solution of the kinetics as discussed in "Kinetics of the transformed volume". In addition, Eq. 21 is also consistent with the type-II growth mechanism for spherical nuclei.

Let us now consider this issue in more detail. For the type II mechanism, the computation reduces to the determination of both radius ($r_0(t)$) and center of mass of the nucleus ($\delta x_N$) at running time $t$. These are estimated as $r_0(t) \cong \frac{\bar{x}_+ - \bar{x}_-}{2}$ and $\delta x_N \cong \frac{\bar{x}_+ + \bar{x}_-}{2}$, where $\bar{x}_+$ and $\bar{x}_-$ are the

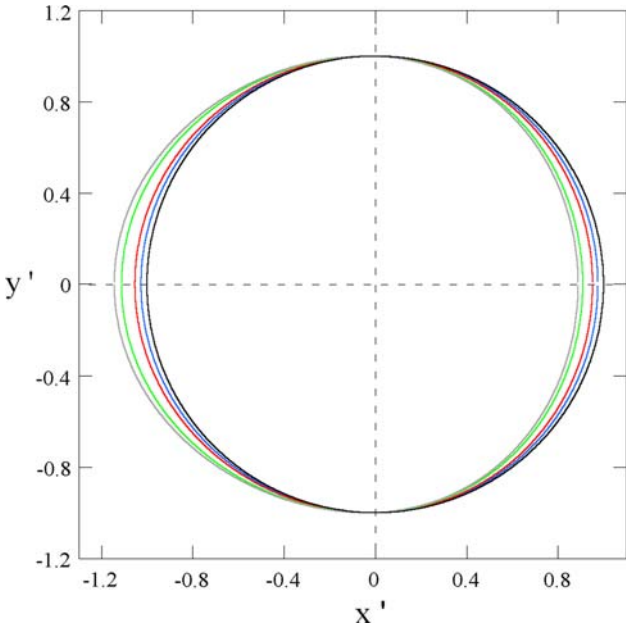


**Fig. 3** Nucleus shape in the case of interface-limited growth (Eqs. 18a, 18b, 20) for several values of the $1/\lambda' = r_0/\lambda$ parameter. $r_0/\lambda = 0$ (*black*); $r_0/\lambda = 0.05$ (*blue*); $r_0/\lambda = 0.1$ (*red*); $r_0/\lambda = 0.2$ (*green*) and $r_0/\lambda = 0.25$ (*grey*). The larger the $r_0/\lambda$ the more negative is the $x$-coordinate of the center of mass of the nucleus. (Color figure online)

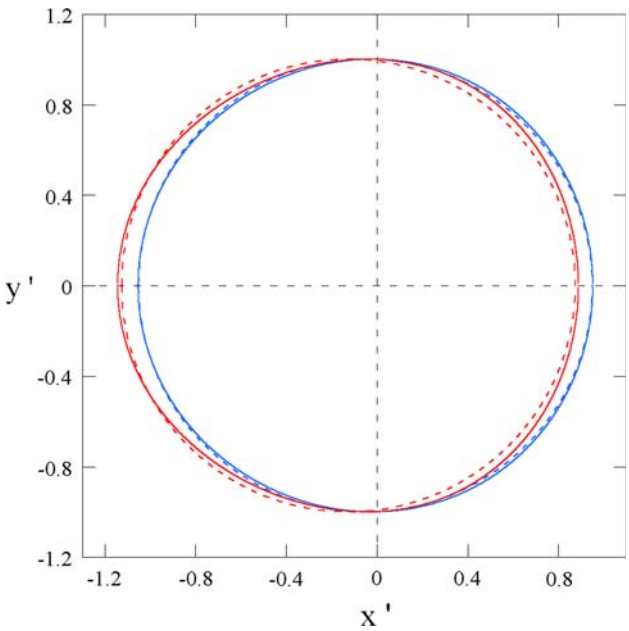


**Fig. 4** Comparison between the shape predicted by Eqs. 18a, 18b, 20 (*solid line*) and the displaced circle given by the approximate Eq. 21 (*dashed line*). The comparison is displayed for $r_0/\lambda = 0.1$ (*blue*) and $r_0/\lambda = 0.25$ (*red*). The larger the $r_0/\lambda$ the more negative is the $x$-coordinate of the center of mass of the nucleus. This holds for both nuclei depicted as *dashed* and *solid lines*. (Color figure online)

positive and negative solutions of Eq. 12 that hold in the local reference frame of the nucleus. By employing Eq. 14 for $\bar{x}_+$ (and a similar equation for $\bar{x}_-$) one obtains $r_0(t) \cong (\lambda - r^*)\sinh(c_0\alpha t/\lambda)$ and $\delta x_N \cong \lambda[1-(1-r^*/\lambda)\cosh(c_0\alpha t/\lambda)]$ which reduces, in the limit $c_0\alpha t/\lambda \ll 1$, to the expressions entering Eq. 21.

Before concluding this section it is worth pointing out that in the case of anisotropic nuclei, the phantom overgrowth is, in general, unavoidable. The conditions, i.e., location and nucleation time, for which this phenomenon occurs, can easily be studied provided the nucleus shape is known. Also, for the unidirectional concentration gradient considered here, and in the limit of a circular nucleus (as given by Eq. 21) only the phantom nuclei located at $x > 0$ could overtake the actual nucleus. To be specific, let us consider an actual nucleus at $x = x_0 = 0$, $y = y_0 = 0$ which starts growing at time $t = \tau_0$ and a phantom nucleus located at $x = x_1$, $y = y_1$ which starts growing at time $t = \tau_1 > \tau_0$. We recall that the $x$-coordinates of the center of the circles of the actual ($a$) and phantom ($p$) nucleus are (Eq. 21) $C_a(t) = -\gamma\frac{r_a^2(t)}{\lambda}$ and $C_p(t) = -\gamma\frac{r_p^2(t)}{\lambda}$, respectively, where $r_a(t) = r_0(t-\tau_0, x_0) = \alpha c(x_0)(t-\tau_0)$ and $r_p(t) = r_0(t-\tau_1, x_1) = \alpha c(x_1)(t-\tau_1)$. Therefore, the overgrowth phenomenon requires the following inequalities to be fulfilled:

$$r_a^2(\tau_1) > y_1^2 + (x_1 - C_a(\tau_1))^2 \tag{22a}$$

$$(r_a(\bar{t}) - r_p(\bar{t}))^2 < (\overline{OO'})^2 \tag{22b}$$

where $(\overline{OO'})^2 = \left(x_1 + C_p(\bar{t}) - C_a(\bar{t})\right)^2 + y_1^2$. Inequalities (a) and (b) give, respectively, the conditions for the formation of a phantom and for the overgrowth (see also Fig. 5). By retaining terms up to the first order in $\lambda'^{-1}$, Eqs. 22a, 22b lead to

$$2x_1\left(C_a(\tau_1) + C_p(\bar{t}) - C_a(\bar{t})\right) > \left(r_a(\bar{t}) - r_p(\bar{t})\right)^2 - r_a^2(\tau_1 - \tau_0) \cong 0, \tag{23}$$

which is satisfied for $x_1 > 0$ since $\bar{t} > \tau_1 > \tau_0$ and the condition $c(x_0) \cong c(x_1)$ can be assumed to hold.

## Kinetics of the transformed volume: site saturation

The eventual aim of this section is to study the kinetics of nucleation and growth reactions in the case of interface-limited growth and simultaneous nucleation (or site saturation), where all nuclei start growing at $t = 0$. Nucleus shape is described by Eq. 21 that holds true provided $\lambda'^{-1} < 1$. Accordingly, for two-dimensional growth the kinetics of the transformed volume reads

$$\ln[1-\xi(t,X_0)] = -N\int_0^{2\pi} \mathrm{d}\theta \int_0^{\bar{r}(\theta,t,X_0)} r\mathrm{d}r = -\frac{N}{2}\int_0^{2\pi} \bar{r}^2 \mathrm{d}\theta, \tag{24}$$

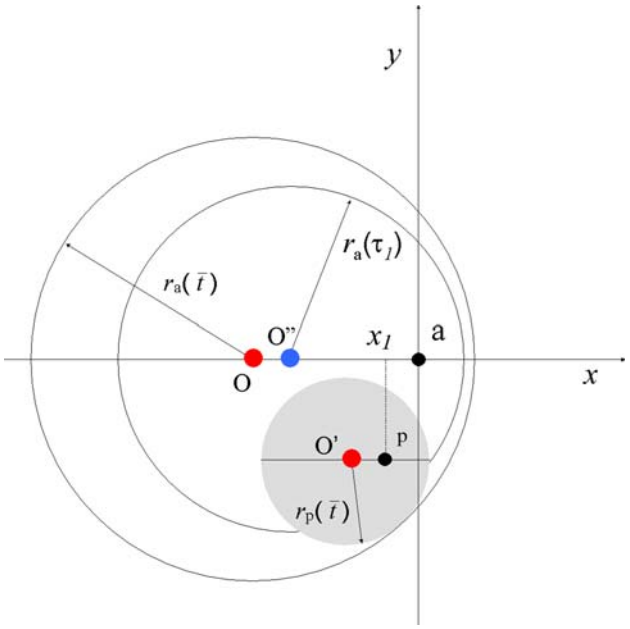


**Fig. 5** Sketch of the overgrowth process in the case of anisotropic growth. According to Eq. 21 nuclei are "displaced circles". In the figure, $a$ and $p$ stand for the nucleation centers of the *actual* and *phantom* nuclei, respectively. The birth time of the phantom is $\tau_1$. O and O′ are, respectively, the circle centers of the actual and of the phantom nuclei at time $\bar{t}$. O″ is the circle center of the actual nucleus at time $\tau_1$ ($\tau_1 < \bar{t}$). The phantom overtakes the actual nucleus at time $\bar{t}$

where $X_0$ is the $x$-component of $\boldsymbol{R}_0$ and the density of nuclei, $N$, is taken as constant.

From Eq. 21 one gets

$$r^2 \cong r_0^2 + 2x\delta x_N, \tag{25}$$

where $r_0 = r_0(t-\tau, x_N) = \alpha c(x_N)(t-\tau)$ and $\delta x_N = -\gamma\frac{r_0^2}{\lambda}$ is the coordinate of the circle center in the nucleus reference frame. By recalling that $x = -r\cos\theta$ Eq. 25 becomes

$$r^2 \cong r_0^2 + 2r\gamma\frac{r_0^2}{\lambda(x_N)}\cos\theta, \tag{26a}$$

where the coordinate of the nucleus center is (see also Fig. 1)

$$x_N = X_0 + r\cos\theta. \tag{26b}$$

The extreme of integration, $\bar{r}$, is therefore obtained by solving the system of Eqs. 26a, 26b in the unknown $r$ at $\tau = 0$, i.e., for $r_0 = \alpha c(x_N)t$.

In order to obtain a manageable analytical solution of the kinetics, let us consider a specific expression for the concentration profile according to $c(x) \propto e^{-x/\lambda}$ where $\lambda$ is constant. Under this circumstance in Eq. 26a, $\lambda(x_N) = -\frac{c(x_N)}{c'(x_N)} \equiv \lambda$. Furthermore, by Taylor expanding the solution of the second order Equation (Eq. 26a) in $\lambda'^{-1}$ and using $c(x_N) \cong c(X_0)\left(1 - \frac{r\cos\theta}{\lambda}\right)$ one gets

$$\bar{r} \cong \bar{r}_0\left[1 - \frac{\bar{r}}{\lambda}\cos\theta + \gamma\frac{\bar{r}_0}{\lambda}\cos\theta\right], \tag{27a}$$

where $\bar{r}_0 = \alpha c(X_0)t$ and only first order terms in $1/\lambda$ have been retained. Therefore,

$$\bar{r} \cong \bar{r}_0\left[1 + \gamma\frac{\bar{r}_0}{\lambda}\cos\theta\right]\left[1 + \frac{\bar{r}_0}{\lambda}\cos\theta\right]^{-1} \tag{27b}$$

which implies, $\bar{r}^2 \cong \bar{r}_0^2\left[1 + 2\gamma\frac{\bar{r}_0}{\lambda}\cos\theta\right]\left[1 + 2\frac{\bar{r}_0}{\lambda}\cos\theta\right]^{-1}$. By evaluating the integral of Eq. 24, the *local* kinetics becomes

$$\ln[1 - \xi(t, X_0)] = -\xi_e(t, X_0), \tag{28a}$$

with the local extended volume

$$\xi_e(t, X_0) = N\pi\bar{r}_0^2(t)\left[\gamma + (1-\gamma)\left(1 - \left(\frac{2\bar{r}_0(t)}{\lambda}\right)^2\right)^{-1/2}\right]. \tag{28b}$$

Alternatively, Eq. 28b can be rewritten as

$$\xi_e(t, X_0) = \bar{\xi}_e(t)\left[\gamma + (1-\gamma)\left(1 - \frac{4\bar{\xi}_e(t)}{\pi N\lambda^2}\right)^{-1/2}\right] \tag{28c}$$

where $\bar{\xi}_e(t) = N\pi\bar{r}_0^2(t)$ is the local extended volume in the zero-order approximation (i.e., computed at the local composition $c(X_0)$ and for $\lambda \to \infty$).

In analogy with the two-dimensional case, the computation above can also be applied to the three-dimensional growth by conjecturing that, for a small degree of inhomogeneity, nuclei are "displaced spheres", with respect to the nucleation center. The computation simplifies through a suitable choice of the polar axis that is oriented parallel to the concentration gradient. It is possible to show that Eq. 27b holds for this case as well, and the local extended volume becomes

$$\begin{aligned}\xi_e(t, X_0) &= N\frac{1}{3}\int_0^{2\pi} \mathrm{d}\phi \int_{-1}^{1} \bar{r}^3 \mathrm{d}\cos\theta \\ &\cong \frac{2\pi}{3}N\bar{r}_0^3\int_{-1}^{1}\left(1 + 3\gamma\frac{\bar{r}_0}{\lambda}\cos\theta\right)\left(1 + 3\frac{\bar{r}_0}{\lambda}\cos\theta\right)^{-1}\mathrm{d}\cos\theta \\ &= \frac{\bar{\xi}_e}{2}\left[\frac{\lambda}{3\bar{r}_0}(1-\gamma)\ln\left(\frac{1 + 3\bar{r}_0/\lambda}{1 - 3\bar{r}_0/\lambda}\right) + 2\gamma\right],\end{aligned} \tag{29}$$

where $\bar{\xi}_e = \frac{4\pi}{3}N\bar{r}_0^3$. Also in this case, for $\lambda \to \infty$, Eq. 29 gives the KJMA formula at the local composition [29, 30]: $\xi(t, X_0) = 1 - e^{-\bar{\xi}_e(t, X_0)}$. It is worth pointing out that the whole transformed volume is obtained through the average $\xi(t) = \frac{1}{h}\int_0^h \xi(t, X)dX$, where $h$ is the sample thickness [26, 30].

The behavior of the local transformed fraction is shown in Fig. 6a, b for two- and three-dimensional transitions,

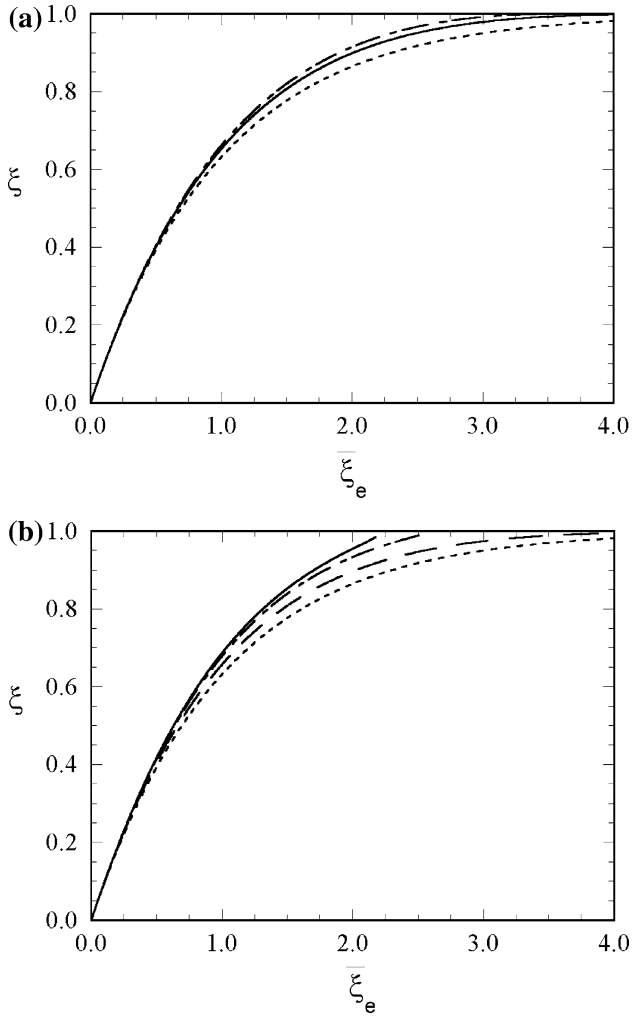


**Fig. 6** Kinetics of the transformed fraction for two-dimensional (panel **a**) and three-dimensional (panel **b**) growths in the case of site saturation. The kinetics is plotted as a function of the local extended volume. In both panels the *dashed line* is the KJMA equation for the (local) growth rate at the point where the transition is studied ($\boldsymbol{R}_0$). Panel **a** $\Gamma_{2D} = 20$ (*solid line*), $\Gamma_{2D} = 15$ (*dash-dotted line*). Panel **b** $\Gamma_{3D} = 140$ (*long-dashed line*); $\Gamma_{3D} = 70$ (*dash-dotted line*); $\Gamma_{3D} = 60$ (*solid line*)

respectively, as a function of the extended fraction, $\bar{\xi}_e$, and for several figures of $\Gamma_{2D} = \pi N\lambda^2$ (two-dimensional growth) and $\Gamma_{3D} = \frac{4}{3}\pi N\lambda^3$ (three-dimensional growth). As can be seen, the present approach predicts an enhancement of the reaction rate when compared to that computed in the zero-order approximation, namely for a homogeneous system with composition just equal to the local value $c(X_0)$. This result can be understood by noting that the dimensionless extended volume is equal to the number of nuclei which lie in the region encompassed by the $\bar{r}(\theta)$ curve. For two-dimensional growth this region is displayed in Fig. 7 for some values of $\lambda'^{-1}$ and its area is found to be greater than $\pi\bar{r}_0^2$.

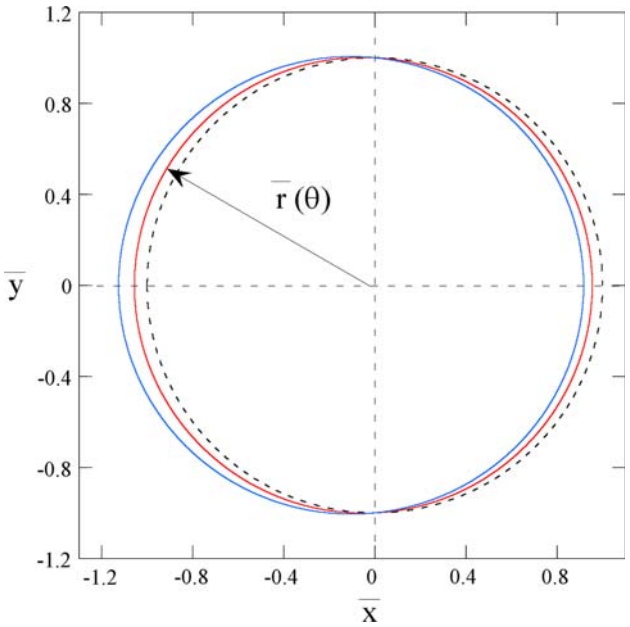


**Fig. 7** Normalized radius of influence, $\bar{r}(\theta) = \bar{r}(\theta)/\bar{r}_0$, in the case of two-dimensional transitions for $1/\lambda' = 0.1$ (*solid line*, *red curve*), $1/\lambda' = 0.2$ (*solid line*, *blue curve*). The circle $\bar{r}(\theta) = \bar{r}_0$, corresponding to the homogeneous system ($1/\lambda' = 0$), is shown as *dashed line*. The smaller the $\lambda'$ value the more the displacement of the curve from the circle of radius $\bar{r}_0$. The dimensionless extended area is equal to the number of nuclei within the area encompassed by this curve. (Color figure online)

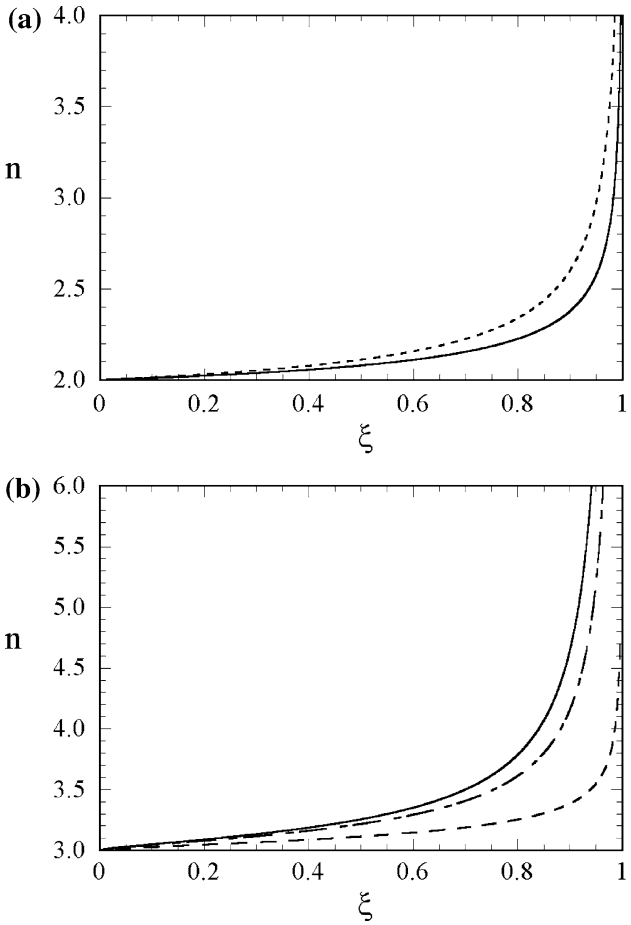


**Fig. 8** Avrami's exponent for two-dimensional (panel **a**) and three-dimensional (panel **b**) growths. Panel **a** $\Gamma_{2D} = 20$ (*solid line*); $\Gamma_{2D} = 15$ (*dashed line*). Panel **b** $\Gamma_{3D} = 140$ (*dashed line*); $\Gamma_{3D} = 70$ (*dash-dotted line*); $\Gamma_{3D} = 60$ (*solid line*)

The behavior of the Avrami exponent as a function of the local transformed volume $\xi(t, X_0)$, is shown in Fig. 8a, b. It is computed through the expression $n(\xi) = D\frac{d\ln\xi_e}{d\ln\xi_e}$ ($D = 2, 3$) that is found to be larger than 2 and 3 for the two- and three-dimensional growths, respectively. In fact, for linear growth of the nuclei and simultaneous nucleation the KJMA formula gives Avrami's exponents that are just equal to D. It is worth noting that Avrami's exponents larger than 3 have been obtained from experimental data on the crystallization of $Fe_{33}Zr_{67}$ alloy for $0.1 < \xi < 0.7$ [30] and of $Zr_{80}Ni_{20}$ alloy for $0.15 < \xi < 0.5$ [33]. The anomalous behavior of the exponent has been ascribed, in reference [30], to the inhomogeneity of the sample.

A detailed study on the behavior of the Avrami exponent in diffusion controlled growth of primary crystallization has been presented in reference [34]. The modeling, which refers to a homogeneous system, shows that this exponent is a decreasing function of the fraction of transformed volume and, moreover, it is suitable for interpreting experimental data on the amorphous to crystalline transitions in alloys. On the other hand, in the case of interface controlled growth, experimental data of eutectic crystallization of alloys give Avrami's exponents that are nearly constant [35]. The present computation therefore indicates that in a non-homogeneous system the Avarmi exponent exhibits a behavior which, in principle, should be discernible from those typical of a homogeneous medium.

In order to describe experimental kinetics, a phenomenological equation has been proposed that includes, as limiting case, the KJMA solution. In differential form the equation reads

$$\frac{d\xi}{d\tilde{\xi}} = (1-\xi)^{\kappa} \tag{30a}$$

or, in integral form,

$$\xi = 1 - \left[1 + (\kappa - 1)\tilde{\xi}\right]^{\frac{1}{1-\kappa}}, \tag{30b}$$

where $\tilde{\xi}$ plays the role of extended volume and $\kappa$ is the impingement parameter [29]. The KJMA formula is obtained in the limit $\kappa = 1$. In order to apply Eq. 30a to the inhomogeneous case discussed so far, it is reasonable to identify $\tilde{\xi}$ with the value expected for a homogeneous medium, and computed at the point where the transition

occurs, that is the $\bar{\xi}_e$ quantity. Furthermore, by using the definition above on the dynamical Avrami's exponent, $n$, one gets

$$\kappa = 1 + \frac{\ln(n\xi_e) - \ln(D\bar{\xi}_e)}{\ln(1-\xi)}. \quad (31)$$

The behavior of $\kappa$ is displayed in Fig. 9a, b as a function of the local value of the transformed volume for several values of $\lambda'$. As can be seen the impingement factor is, approximately, uniform on $\xi$, and it is lower than unity in the entire range of $\xi$. The value of the parameter $1/\lambda'$, is reported in Fig. 10 as a function of the transformed volume for the two- and three-dimensional growth processes of Fig. 6a, b. It turns out that up to a reaction extent of 85% the expansion parameter is lower than 0.1.

The model kinetics could also be employed for describing the initial stage of the metal dusting. As anticipated in the "Introduction" section, this phenomenon involves metal surfaces in carburizing atmosphere,

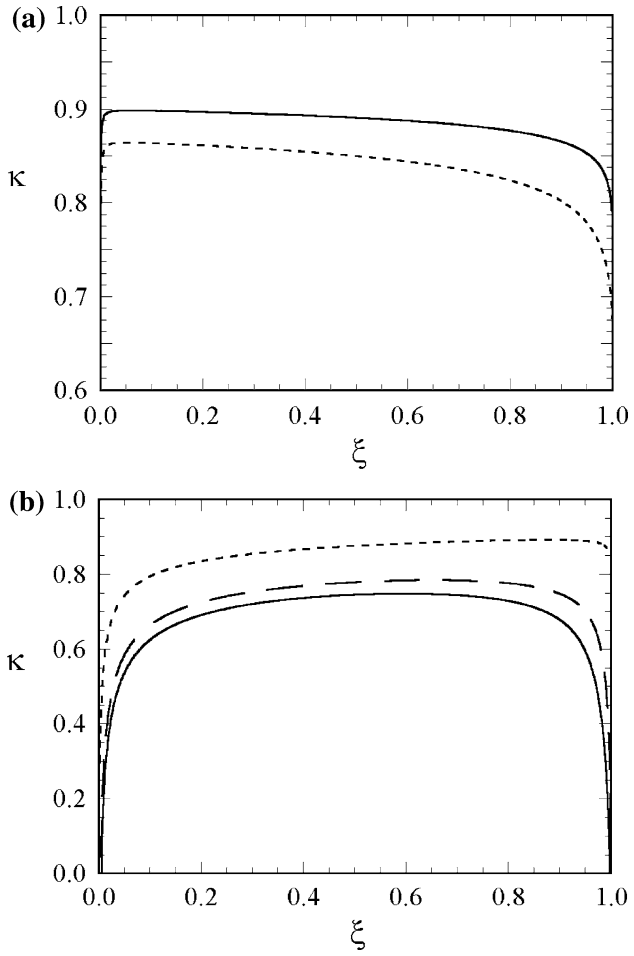


**Fig. 9** Dynamical impingement factor for the kinetics of Fig. 6. Panel **a** $\Gamma_{2D} = 20$ (*solid line*); $\Gamma_{2D} = 15$ (*dashed line*). Panel **b** $\Gamma_{3D} = 140$ (*dashed line*); $\Gamma_{3D} = 70$ (*long-dashed line*); $\Gamma_{3D} = 60$ (*solid line*)

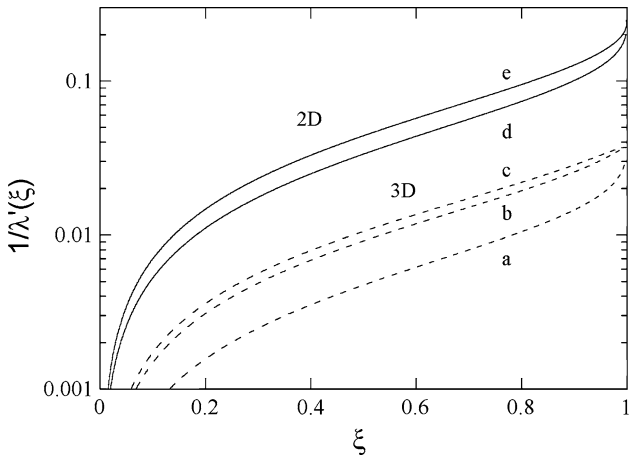


**Fig. 10** Behavior of the parameter, $1/\lambda'(t) = r_0(t)/\lambda$, as a function of the local transformed fraction for the kinetics of Fig. 6. Curve (*a*) $\Gamma_{3D} = 140$; (*b*) $\Gamma_{3D} = 70$; (*c*) $\Gamma_{3D} = 60$; (*d*) $\Gamma_{2D} = 20$; (*e*) $\Gamma_{2D} = 15$

containing CO and/or hydrocarbons. The initial stage of the reaction is the diffusion of C atoms from the surface into the metal, leading to the formation of metal–carbon solid solution. In the specific case of iron, cementite is the intermediate into which the subsequent growth of graphite takes place [27]. The nucleation and growth of cementite is therefore expected to occur under a concentration gradient of C atoms. By assuming quasi-steady state conditions the concentration profile of C into the metal is in accord with the exponential decay $c(x) \propto c_s e^{-x/\lambda}$, where $\lambda = \sqrt{D\tau}$ is the diffusion length and $c_s$ the concentration of C atoms at the surface. The characteristic time $\tau$ (life time), is the inverse of the probability, per unit time, that a C-atom be captured by the cementite nuclei. Accordingly, Eq. 29 can be applied to describe the nucleation and growth of the intermediate phase with the local quantity $\frac{\bar{r}_0}{\lambda} = \frac{1}{\lambda}\alpha c_s e^{-X_0/\lambda} t$ which scales as $\frac{\bar{r}_0}{\lambda} \propto \frac{D^{1/2} t c_s}{\tau^{1/2}\rho} e^{-X_0/\lambda}$.

As far as the phase transformation in two-dimension is concerned, it is worth quoting the experiment of diamond growth on silicon surface, by using the ultra short bias enhanced plasma deposition technique (USBEN) [36]. The authors present a detailed analysis of the physical quantities which characterize the growth. In order to gain an insight into the homogeneity of the system, cartography of the nucleation density, surface coverage and mean island size have been measured and show that the growth conditions are not uniform throughout the surface. Therefore, the model could be employed to compute the fractional coverage of silicon by diamond by using both nucleation and growth rates which depend upon position. Moreover, the experimental data indicates that the length scale over which the growth parameters change, is longer that the mean nucleus size and this makes valid the first order expansion employed in the modeling.

It is worth stressing that although the present model has been developed in the specific case of an inhomogeneous concentration profile, the analytical results of Eqs. 28, 29, appear to be quite general. In fact, these kinetics hold provided that $\frac{d\Re}{dt} \propto e^{-x/\lambda}$(Eq. 10, See Footnote 1.) where this behavior can be due to either a temperature or a concentration gradient. The present approach can also be employed to deal with any concentration (or temperature) profile. In this case, however, the dependence of $\lambda(x_N) = -\frac{c(x_N)}{c'(x_N)}$ on nucleus location has to be duly taken into account in Eq. 26a.

## Conclusions

A model has been developed for dealing with nucleation and growth reactions in inhomogeneous systems. The kinetic equation is found to resemble the KJMA formula where the local "extended volume" is now a multiple integral over the birth time of the nuclei, the time at which the transformation of the point may occur, and the angular variables. In the case of small degrees of inhomogeneity, the kinetics is employed for estimating first order corrections to the local KJMA kinetics. For this purpose, the case of site saturation and interface-limited growth has been investigated. In two-dimensional growth the shape of the nucleus is found to be well described by a displaced circle and this allows one to compute, analytically, the local kinetics. The same approach has also been applied to investigate three-dimensional growth. First order corrections to the KJMA formula lead, in both two- and three-dimensional cases, to an increase in the reaction rate. This is highlighted through the analysis of the Avrami exponent that is found to be greater than 2 and 3 for two- and three-dimensional transitions, respectively. The analysis of the impingement factor gives values that are lower than one and approximately constant in time. These values, however, depend on the choice of the local "extended volume" that enters the phenomenological equation. Here, the impingement factor is referred to the extended volume computed in the zero-order approximation.

## References


1. Schmalzried H (1974) Solid state reactions. Academic Press, INC, New York, London
2. Cahn RW Haasen P (1983) In: Cahn RW, Haasen P (eds) Physical metallurgy part II. North Holland Physics Publishing, Amsterdam, Oxford, New York, Tokyo
3. Crespo D, Pradell T (1996) Phys Rev B 54:3101
4. Rickman JM, Tong WS, Barmak K (1997) Acta Mater 45:1153
5. Pineda E, Pradell T, Crespo D (2001) J Non-Cryst Solids 287:88
6. Farjas J, Roura P (2008) Phys Rev B 78:144101
7. Klikovits J, Schmid M, Gustafson J, Mikkelsen A, Resta A, Lundgren E, Andersen JN, Varga P (2006) J Phys Chem B 110
8. Kolmogorov AN (1937) Bull Acad Sci URSS 3:355
9. Johnson WA, Mehl RF (1939) Trans Am Inst Min Metall Pet Eng 135:416
10. Avrami M (1939) J Chem Phys 7:1103
11. Avrami M (1940) J Chem Phys 8:212
12. Fanfoni M, Tomellini M (2005) J Phys Condens Matter 17:R571
13. Rios PR, Oliveira JCPT, Oliveira VT, Castro JA (2006) Mater Res 9:165
14. Uebele P, Hermann H (1996) Model Simul Mater Sci Eng 4:203
15. Birnie DP, Weinberg MC (1995) J Chem Phys 103:3742
16. Weinberg MC, Birnie DP (1996) J Non-Cryst Solids 202:290
17. Pusztai T, Gránásy L (1998) Phys Rev B 57:141
18. Kooi BJ (2004) Phys Rev B 70:224108
19. Burbelko AA, Fraś E, Kapturkiewicz W (2005) Mater Sci Eng A 413:429
20. Shepilov MP (2004) Glass Phys Chem 30:291
21. Shepilov MP, Baik BS (1994) J Non-Cryst Solids 171:141
22. Farjas J, Roura P (2007) Phys Rev B 75:184112
23. Levine LE, Lakshmi Narayan K, Kelton KF (1997) J Mater Res 12:124
24. Berg BA, Dubey S (2008) Phys Rev Lett 100:165702
25. Todinov MT (2000) Acta Mater 48:4217
26. Alekseeckin NV (2001) J Phys Condens Matter 13:3083
27. Grabke HJ (2003) Mater Corros 54:736
28. Starink MJ (2001) J Mater Sci 36:4433. doi:10.1023/A:1017974517877
29. Starink MJ (2004) Int Mater Rev 49:191
30. Sun NX, Liu XD, Lu K (1996) Scripta Mater 34:1201
31. Avrami M (1941) J Chem Phys 9:177
32. Fanfoni M, Tomellini M (1998) Il Nuovo Cimento 20:1171
33. Asahi N, Miyashita A (1988) Jpn J Appl Phys 27:875
34. Pradell T, Crespo D, Clavaguera N, Clavaguera-Mora MT (1998) J Phys Condens Matter 10:3833
35. Zhou F, He K, Sui M, Lai Z (1994) Mater Sci Eng A 181/182:1419
36. Saada S, Barrat S, Bauer-Grosse E (2000) Diam Relat Mater 9:300